forests

MDPI

Article

Dynamic Model for *Caragana korshinskii* Shrub Aboveground Biomass Based on Theoretical and Allometric Growth Equations

Xuejuan Jin [1], Hao Xu [2,*], Bo Wang [1] and Xiaohua Wang [1]

[1] School of Agriculture, Ningxia University, Yinchuan 750021, China
[2] School of Economics and Management, Ningxia University, Yinchuan 750021, China
* Correspondence: xhao0202@163.com

Abstract: As one of the ways to achieve carbon neutralization, shrub biomass plays an important role for natural resource management decision making in arid regions. To investigate biomass dynamic variations of *Caragana korshinskii*, a typical shrub found in the arid desert area of Ningxia, northwest China, we combined a nonlinear simultaneous (NLS) equation system with theoretical growth (TG) and allometric growth (AG) equations. On the basis of a large biomass survey dataset and analytical data of shrub stems, four methods (NOLS, NSUR, 2SLS, and 3SLS) of the NLS equations system were combined with the TG and AG equations. A model was subsequently established to predict the AGB growth of *C. korshinskii*. The absolute mean residual (*AMR*), root mean system error (*RMSE*), and adjusted determination coefficient (adj-R^2) were used to evaluate the performance of the equations. Results revealed that the NSUR method of the NLS equations had better performance than other methods and the independent equations for BD and H growth and AGB. Additionally, the NSUR method exhibited extremely significant differences ($p < 0.0001$) when compared with the equations without heteroscedasticity on the basis of the likelihood ratio (LR) test, which used the power function (PF) as the variance function. The NSUR method of the NLS equations was an efficient method for predicting the dynamic growth of AGB by combining the TG and AG equations and could estimate the carbon storage for shrubs accurately, which was important for stand productivity and carbon sequestration capacity.

Keywords: theoretical growth equation; allometric growth equation; nonlinear simultaneous equations system; heteroscedasticity; *Caragana korshinskii* shrub

Citation: Jin, X.; Xu, H.; Wang, B.; Wang, X. Dynamic Model for *Caragana korshinskii* Shrub Aboveground Biomass Based on Theoretical and Allometric Growth Equations. *Forests* **2022**, *13*, 1444. https://doi.org/10.3390/f13091444

Academic Editors: Tianxiang Yue and Yifu Wang

Received: 20 July 2022
Accepted: 7 September 2022
Published: 8 September 2022

1. Introduction

Biomass is investigated when studying the carbon storage of forest ecosystems, as it is an important indicator of stand productivity and carbon sequestration capacity and plays an indicative role in forest quality assessment [1,2]. Shrubs are indispensable and important species in the forest ecosystem and play essential roles in ecological processes. Aboveground biomass (AGB) is expressed on an area basis and is central to many ecological processes and services provided by shrublands [3]. It is the main forest vegetation type found in the arid aeolian sand regions (AASRs) of China. Shrubs are widely used for ecological protection and restoration measures and reconstruction projects due to their well-developed root systems and remarkable abilities in wind and sand fixation, soil and water conservation, and drought resistance. Thus, studying shrub biomass is of great importance for ecosystem restoration, regeneration, and security in the AASRs [4].

In recent years, scholars have constructed many biomass models [5,6]. The first study on biomass was conducted in 1876 when Ebermeryer in Germany investigated the dry matter productivity of the Bavarian Forest by measuring the amount of leaf litter and wood weight of certain tree species. The earliest measurements and studies on shrub biomass have been traced back to the early 1960s [7,8]. Lufafa et al. [9] studied the shrub

biomass model and obtained good results. However, the model was mostly static and not dynamic [10]. Due to differences in species biomasses and environmental conditions, such as temperature, precipitation, and elevation, application of the shrub biomass prediction model has been limited [11,12]. For shrub forests, there is no unified standard by which the method is used to establish biomass models.

Due to the increasing importance of forests as carbon sinks for carbon neutrality, there is a growing need for new models to address the dynamic biomass model [13]. The dynamic biomass model uses age as the independent variable and is convenient for the dynamic assessment of forest biomass. The model is governed by an underlying forest growth mechanism controlled by a variety of ecological processes [14], which has great predictive abilities for forest production and contributions. However, this model has been seldom applied in forest growth, as a single dimension of time is needed to obtain forest biomass. Existing dynamic biomass models have often been built using the space-for-time substitution method to obtain forest biomass data at different stages in the same site [15]. Thus, it may lead to erroneous conclusions when using the space-for-time substitution assumption for a spatial regression analysis on static data with only spatial variation while studying ecological processes in static spatial datasets [16]. Realistically, it is difficult to ensure the consistency of site conditions (i.e., elevation, slope, and slope aspects) at different stages, especially in nonstationary environments [17]. Moreover, it is necessary to acquire a mass of data, which limits the development and construction of dynamic biomass models [18].

A potential solution for these limitations is the application of nonlinear simultaneous (NLS) equations [19], including the theoretical growth (TG) equations of basal diameter (BD) and/or height (H) and the allometric growth (AG) equations of AGB as functions of the BD and/or H of shrubs. The TG equation describes the age-dependent growth of an organism or population, which reflects the regularity of the growth of some organisms [20,21]. It is characterized by logic and the biological significance of parameters. Tree-ring widths are effective for the prediction of BD and H growth processes [22–24]; TG models have been presented in many forms [25–29], including the Logistic, Richards, Korf, Gompertz, and Mitscherlich functions. Additionally, as it is commonly used to predict forest biomass, the AG equation typically uses nonlinear power-law forms that predict AGB and the BD and/or H of shrubs as the independent variables. Due to the simplicity and high efficiency, AG equations have been widely used to accurately estimate forest biomass and carbon storage, as well as to study degraded forest ecosystems [11,30].

Caragana korshinskii belongs to the *Caragana* genus and has a developed root system, vigorous growth, wide adaptability, and strong stress resistance [31]. As a major forest vegetation type found in the AASRs of Ningxia, northwest China, *C. korshinskii* has played a positive role in improving the ecological environment of the sandy area and promoting the economic construction and development of local animal husbandry. In this study, dynamic AGB models of *C. korshinskii* in the AASRs were established using the NLS equation method using the optimal TG equations of BD and H, which were selected by fitting, and the AG equations of AGB, which were constructed using BD and/or H as the independent variables on the basis of a large biomass dataset. The objectives of this paper are to (a) describe the dynamic growth of AGB for *C. korshinskii* on the basis of dynamic AGB model and (b) estimate biomass and carbon stock for native desert shrub in the AASRs. The novelty of the study is to construct the dynamic growth model of AGB for *C. korshinskii* shrubs using the NLS equations. The dynamic AGB model will enhance our understanding of ecological adaptation strategies and the evolutionary mechanisms of lemon populations in the AASRs, as well as serve as a useful resource for developing and utilizing *C. korshinskii*.

2. Materials and Methods

2.1. Study Area

The study area is located in the AASRs, Yanchi County (37°4′–38°10′ N, 106°30′–107°47′ E), Ningxia Province, northwestern China. It is a typical zone consisting of agricultural to pastoral areas with a temperate continental climate [32]. The annual average temperature is 7.7 °C, the mean annual precipitation is 297 mm, and the annual evaporation is 2100 mm [33,34]. The soil consists mainly of sierozem and aeolian sand. Due to sparse precipitation, large evaporation, and a serious shortage of water resources in the county, the tree species mainly include grassland, sandy, and halophyte vegetation, including *C. korshinskii*, *Nitraria sibirica*, and *Hedysarum scoparium*.

2.2. Data Collection

C. korshinskii is an important shrub species for soil and water conservation and sand-fixation afforestation in northwest and northeast China. It is a perennial legume shrub with strong drought resistance and has a planting area that exceeds 40% [35,36]. A total of 39 temporary sample plots of *C. korshinskii* were selected in the study area (Figure 1). Sample plots were square and varied in size, ranging from 100 to 400 m^2. The BD (mm) at 10 cm aboveground, H (m), crown width (m), and total number of stems (N) of all shrubs in the sample plot were measured. Then, two or three individual shrubs from each sample plot were selected for analysis on the basis of the average BD, H, crown width, and number of stems. A total of 87 individual shrubs were collected. The aboveground parts were collected, and dry samples of the stems and leaves were transported to the laboratory at a constant 85 °C and constant weight. We calculated the moisture content of each component according to the relationship between the fresh and dry mass of each sample, then calculated the dry matter mass of each part of the sample and added each part to obtain the AGB of *C. korshinskii* (Table 1). Three to five stems with the largest BD and H from individual shrubs were selected, segmented into 20 cm lengths, and cut into disks, which were scanned using WinDENDRO software to count the number of annual rings and measure the diameter and H in increments.

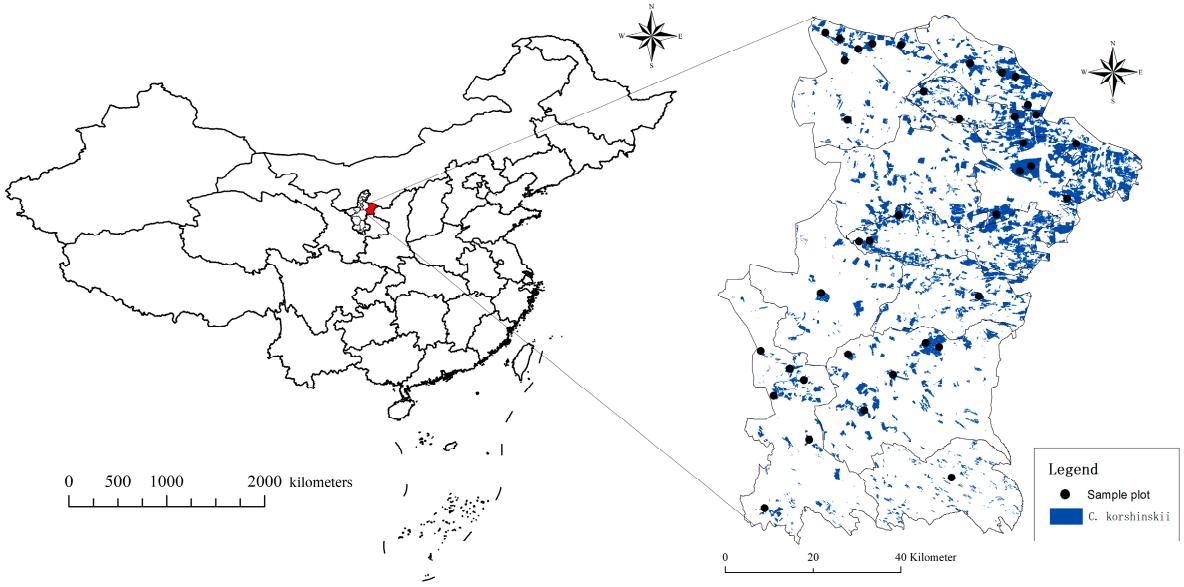

Figure 1. Map (ArcGIS v10.4.1) of the study area located in Ningxia Province, China.

Table 1. Summary statistics used for the data analysis.

Factors	Number of Individual Shrubs	Mean	Minimum	Maximum	Standard Deviation
Age (year)	87	18.8	3.00	31.00	7.19
Basal diameter (mm)	87	13.3	1.90	22.60	5.29
Height (m)	87	2.2	0.30	3.40	0.69
Total number of stems (N)	87	21.3	6.00	59.00	11.22
AGB (kg)	87	5.8	0.37	12.61	3.17

2.3. Test of Data Normality

The Shapiro–Wilk test was used to test the normality of BD growth, H growth, and AGB data (Table 2). Because the data showed non-normal distribution ($p < 0.05$), the *gnls* function in R was applied to establish the generalized nonlinear (GNL) models of BD growth, H growth, and AGB.

Table 2. Results of the data normality test.

Data	*SW* Value	*p*-Value
BD growth	0.9505	0.0022
H growth	0.9667	0.0243
AGB	0.9364	0.0003

Note: *SW* is the Shapiro–Wilk test statistic. $p < 0.05$ indicates non-normal distribution.

2.4. Biomass Model Construction

2.4.1. Theoretical Growth Equation

As a model that describes changes in biometric variables (BD and H) with age, the TG equation reflects the basic law of shrub stand growth with certain assumptions based on biological characteristics. Differential or calculus equations of the total growth curve of the shrub were established, and the initial or boundary conditions were substituted to obtain the special solution of the differential equations. Currently, the most widely used TG equations are the five aforementioned functions (Table 3).

Table 3. The five TG equations.

Equations	Formulas
Gompertz	$I = a_{1,2}e^{-b_{1,2}e^{-c_{1,2}A}}$
Logistic	$I = \frac{a_{1,2}}{1+b_{1,2}e^{-c_{1,2}A}}$
Mitscherlich	$I = a_{1,2}\left(1 - b_{1,2}e^{-c_{1,2}A}\right)$
Richards	$I = a_{1,2}\left(1 - e^{-c_{1,2}A}\right)^{b_{1,2}}$
Korf	$I = a_{1,2}e^{-b_{1,2}/A^{c_{1,2}}}$

Note: A is the shrub age; I is the increments of BD and H at A year; a_1, b_1, and c_1 are model parameters for BD growth; and a_2, b_2, and c_2 are model parameters for H growth.

2.4.2. Allometric Growth Equation

The AG equation is used to estimate shrub biomass with easily measurable factors, such as BD and/or H, which saves manpower and material resources and is less destructive when compared to the direct harvesting method [37]. Three AG equations of AGB were established in the study (Table 4).

Table 4. The three AG equations.

Equations	Independent Variables	Model Parameters
$W = a_3(n\mathrm{BD}_m)^{b_3}$	$n\mathrm{BD}_m$	a_3, b_3
$W = a_3(n\mathrm{H}_m)^{b_3}$	$n\mathrm{H}_m$	a_3, b_3
$W = a_3\left((n\mathrm{BD}_m)^2\mathrm{H}_m\right)^{b_3}$	$(n\mathrm{BD}_m)^2\mathrm{H}_m$	a_3, b_3

Note: W is the AGB; n is the number of stems, and BD_m, and H_m are the means of BD and H for an individual shrub, respectively; and a_3 and b_3 are model parameters.

2.4.3. Nonlinear Simultaneous Equations

The TG equations of BD and H with age were established using the five functions (Table 3). The AG equations of AGB were constructed using BD and H as the independent variables and the power function (PF) (Table 4). Then, the best equations for the TG and AG equations were selected after evaluation. Finally, the nonlinear ordinary least square (NOLS), nonlinear seemingly uncorrelated regression (NSUR), two-stage least squares (2SLS), and three-stage least squares (3SLS) methods were used to build a dynamic system of the NLS equations for AGB by combining the best TG and AG equations (Table 5). The formula of the NLS equations in this study is as follows:

$$\begin{cases} BD = f(A) \\ \mathrm{H} = f(A) \\ W = f(BD, H) \end{cases} \quad (1)$$

where f are the best performed equations for BD growth, H growth, and AGB models according to the evaluation indices.

Table 5. The four methods of the NLS system.

Method	Instruments	Objective Function	Covariance of θ
NOLS	No	$\gamma'\gamma$	$\left(X\left(diag(S)^{-1}\otimes\right)X\right)^{-1}$
NSUR	No	$\gamma'\left(diag(S)^{-1}_{OLS}\otimes I_m\right)\gamma$	$\left(X\left(S^{-1}\otimes I_m\right)X\right)^{-1}$
2SLS	Yes	$\gamma'(I_m\otimes V)\gamma$	$\left(X\left(diag(S)^{-1}\otimes I_m\right)X\right)^{-1}$
3SLS	Yes	$\gamma'\left(S^{-1}_{2SLS}\otimes V\right)\gamma$	$\left(X\left(diag(S)^{-1}\otimes V\right)X\right)^{-1}$

Note: γ is a column vector of the residuals for each equation, S is the variance–covariance matrix between the equations ($\widehat{\sigma}_{ij} = \left(\widehat{e}'_i\widehat{e}_j\right)/\sqrt{(T-k_i)\cdot(T-k_j)}$), X is the matrix of the partial derivatives with respect to the coefficients, V is the matrix of the instrument variables $Z(Z'Z)^{-1}Z$, Z is the matrix of the instrument variables, and I_m is the $n\times n$ identity matrix. The NSUR and 3SLS methods require two solutions. The first solution for NSUR is an NOLS solution that obtains the variance–covariance matrix and fits all the equations simultaneously. The second solution for 3SLS uses the variance–covariance matrix from the 2SLS solution and fits all the equations simultaneously.

NOLS is widely used to estimate parameters in a single equation and can thus lead to biased and inconsistent estimations by neglecting correlations among different equations when estimating parameters for each equation [38]. NSUR is an efficient parameter estimation technique when the error components of a system of unrelated equations are correlated [39]. The parameter variances estimated from large samples using NSUR may be less than the parameter variances obtained by NOLS. Meanwhile, 2SLS and 3SLS are adopted for exact identification and overidentified structural equation models. However, 2SLS neglects correlations, and there is some information loss among different equations for one-by-one estimations [40]. As a system method of estimation, 3SLS is effective for the simultaneous estimation of all parameters of different equations, and it considers the correlation of random errors. A system of NLS equations can be written as follows:

$$\varepsilon_t = q(y_t, x_t, \theta),$$

where ε_t is the residuals of y observations and the function evaluated by the coefficient estimates.

$$z_t = Z(x_t)$$

2.5. Heteroscedasticity Test and Elimination

The existence of heteroscedasticity in models makes parameter estimation by ordinary regression biased, leading to increased error and parameter variation coefficients, and thereby affecting the reliability of the models. Alternatively, residual graph analysis is an intuitive and convenient analysis method. When the regression model has heteroscedasticity, the distribution of the points on the residual graph shows a certain trend. In this study, when there was heteroscedasticity, the variance functions, including the PF, exponential function (EF), and constant plus PF (CPF), were used to deal with variance heterogeneity. To compare the models with and without variance functions, the Akaike information criterion (AIC), Bayesian information criterion (BIC), and negative two times the logarithm of the likelihood (−2LL) were used; the smaller the values, the better the model. The formulas of the criterions are as follows:

$$\mathrm{AIC} = 2r - 2\ln(L) \tag{2}$$

$$\mathrm{BIC} = r\ln(n_i) - 2\ln(L) \tag{3}$$

where L is the likelihood of the equations, r is the numbers of model parameters, and n_i is the number of samplers.

2.6. Evaluation of the Models

The TG and AG equations were fit by nonlinear regression. Then, a set of NLS equations combining the TG and AG equations were estimated to obtain the AGB estimation model of *C. korshinskii*. Finally, the variance functions were used to eliminate heteroscedasticity in the fitting. Leave-one-out cross-validation was performed to evaluate two statistical criteria. Three indices, the *AMR*, root mean square error (*RMSE*), and adjusted coefficient of determination (adj-R^2), were calculated as model accuracy metrics. The formulas of the fit statistics are as follows:

$$AMR = \sum_{i=1}^{m}\sum_{j=1}^{n_i}\frac{\left|y_{ij} - \widehat{y}_{ij}\right|}{n_i} \tag{4}$$

$$RMSE = \sqrt{\sum_{i=1}^{m}\sum_{j=1}^{n_i}\frac{\left(y_{ij} - \widehat{y}_{ij}\right)^2}{n_i - r}} \tag{5}$$

$$\text{adj-}R^2 = 1 - (n_i - 1)\left(\frac{\sum_{i=1}^{m}\sum_{j=1}^{n_i}\frac{\left(y_{ij} - \widehat{y}_{ij}\right)^2}{n_i - r}}{\sum_{i=1}^{m}\sum_{j=1}^{n_i}\left(y_{ij} - \overline{y}\right)^2}\right) \tag{6}$$

where $\widehat{y}_{ij}$ is BD growth, H growth, or AGB prediction, and $\overline{y}$ is the average of the observations.

3. Results

3.1. Growth Equations with Generalized Nonlinear Models

3.1.1. Theoretical Growth Equations of Basal Diameter and Height

Five TG equations were constructed to fit the BD and H growth of *C. korshinskii* (Table 6). The results showed that the five equations had good performances when the adj-R^2 was >0.8. However, Gompertz growth equations showed better fitting accuracy than others for both BD and H growth. The *AMR*, *RMSE*, and adj-R^2 were 1.4767, 1.9767, and 0.8636 for the BD growth model, respectively. The *AMR*, *RMSE*, and adj-R^2 were 0.2378, 0.2939, and 0.8248 for the H growth model, respectively. Therefore, the Gompertz equation was selected as the optimal TG equation and built in the follow-up study.

Table 6. Summary of evaluations from fitting BD and H growth of *C. korshinskii* shrubs using GNL regression.

Factors	Equations	*AMR*	*RMSE*	adj-R^2	Factors	Equations	*AMR*	*RMSE*	adj-R^2
BD	Gompertz	1.4767	1.9767	0.8636	H	Gompertz	0.2378	0.2939	0.8248
	Logistic	1.5174	1.9981	0.8606		Logistic	0.2449	0.2993	0.8183
	Mitscherlich	1.5477	2.0381	0.8437		Mitscherlich	0.2498	0.3053	0.8023
	Richards	1.5062	2.0162	0.8467		Richards	0.2426	0.2998	0.8086
	Korf	1.5326	2.0181	0.8521		Korf	0.2473	0.3023	0.8102

3.1.2. Allometric Growth Equation of Biomass

On the basis of easily measurable factors, the total BD ($n\mathrm{BD}_m$), total shrub H ($n\mathrm{H}_m$), and total BD squared multiplied by H ($(n\mathrm{BD}_m)^2\mathrm{H}_m$) were used to establish the AG equations for the AGB of *C. korshinskii* (Table 7). The adj-R^2 of $W = a_3\left((n\mathrm{BD}_m)^2\mathrm{H}_m\right)^{b_3}$ was > 0.8 (adj-R^2 = 0.8014), and the *AMR* and *RMSE* values were both smaller than the other two equations on independent biomass in the AG equations. Therefore, $W = a_3\left((n\mathrm{BD}_m)^2\mathrm{H}_m\right)^{b_3}$ was selected as the best model for the AG equation.

Table 7. Summary of evaluations from fitting AGB of *C. korshinskii* shrubs using GNL regression.

Equations	*AMR*	*RMSE*	adj-R^2
$W = a_3(n\mathrm{BD}_m)^{b_3}$	1.3741	1.6538	0.7304
$W = a_3(n\mathrm{H}_m)^{b_3}$	1.7441	2.1431	0.5473
$W = a_3\left((n\mathrm{BD}_m)^2\mathrm{H}_m\right)^{b_3}$	1.0986	1.4193	0.8014

3.2. Nonlinear Simultaneous Equations of Dynamic Models

In this study, the best performed TG equations of BD and H and the best performed AG equation of AGB were combined using the NOLS, NSUR, 2SLS, and 3SLS methods to construct the NLS equations. Table 8 shows the parameters and evaluation indices after fitting each model. Results revealed that the same estimation parameters and evaluations were obtained by using GNL regression and the NOLS method, which was the same estimation when using the 2SLS and 3SLS methods. However, the NSUR and 2SLS or 3SLS methods showed different outcomes from NOLS. Namely, the NSUR method had better performance than the others. For BD growth of *C. korshinskii* shrubs, the *AMR* and *RMSE* of $\mathrm{BD}_{\mathrm{NSUR}}$ were 1.3481 and 1.8046, which decreased by 9.54% and 9.53% when compared to Equation (4), respectively. The adj-R^2 of $\mathrm{BD}_{\mathrm{NSUR}}$ was 0.9055 and increased by 4.63% when compared to Equation (4). For H growth of *C. korshinskii* shrubs, the *AMR* and *RMSE* of $\mathrm{H}_{\mathrm{NSUR}}$ were 0.2171 and 0.2683, which decreased by 9.53% and 9.54% when compared to Equation (5), respectively. The adj-R^2 of $\mathrm{H}_{\mathrm{NSUR}}$ was 0.8644 and increased by 4.58% when compared to Equation (5). For the AGB of *C. korshinskii* shrubs, the *AMR* and *RMSE* of $\mathrm{AGB}_{\mathrm{NSUR}}$ were 1.0514 and 1.3584, which decreased by 4.49% and 4.48% when compared to Equation (6), respectively. The adj-R^2 of $\mathrm{AGB}_{\mathrm{NSUR}}$ was 0.8246 and increased by 2.82% when compared to Equation (6). Therefore, the NSUR method of the NLS equation system was selected to establish the NLS equations for BD growth, H growth, and AGB.

Table 8. Summary of evaluations from fitting BD and H growth of *C. korshinskii* shrubs using GNL regression and the four methods of the NLS equations.

Method	Equations	Model Parameters								Evaluation Indicator		
		a_1	b_1	c_1	a_2	b_2	c_2	a_3	b_3	*AMR*	*RMSE*	adj-R^2
GNL model	BD growth	32.9515	2.8928	0.0616	—	—	—	—	—	1.4767	1.9767	0.8636
	H growth	—	—	—	3.0767	2.5956	0.1160	—	—	0.2378	0.2939	0.8248
	AGB	—	—	—	—	—	—	0.0163	0.4971	1.0986	1.4193	0.8014
NOLS	BD_{NOLS}	32.9514	2.8928	0.0616	—	—	—	—	—	1.4767	1.9767	0.8636
	H_{NOLS}	—	—	—	3.0767	2.5956	0.1160	—	—	0.2378	0.2939	0.8248
	AGB_{NOLS}	—	—	—	—	—	—	0.0163	0.4971	1.0986	1.4193	0.8014
NSUR	BD_{NSUR}	36.4637	2.9877	0.0572	—	—	—	—	—	1.3481	1.8046	0.9055
	H_{NSUR}	—	—	—	3.2242	2.5382	0.1057	—	—	0.2171	0.2683	0.8644
	AGB_{NSUR}	—	—	—	—	—	—	0.0159	0.4994	1.0514	1.3584	0.8246
2SLS	BD_{2SLS}	33.3535	3.4320	0.0689	—	—	—	—	—	1.5388	2.0598	0.8519
	H_{2SLS}	—	—	—	2.9674	2.7336	0.1280	—	—	0.2386	0.2949	0.8235
	AGB_{2SLS}	—	—	—	—	—	—	0.2391	0.2758	1.4247	1.8406	0.6661
3SLS	BD_{3SLS}	33.3535	3.4320	0.0689	—	—	—	—	—	1.5388	2.0598	0.8519
	H_{3SLS}	—	—	—	2.9674	2.7336	0.1280	—	—	0.2386	0.2949	0.8235
	AGB_{3SLS}	—	—	—	—	—	—	0.2391	0.2758	1.4247	1.8406	0.6661

Note: BD_{NOLS}, H_{NOLS} and AGB_{NOLS} are the BD growth, H growth, and AGB equations with NOLS method, respectively; BD_{NSUR}, H_{NSUR} and AGB_{NSUR} are the BD growth, H growth, and AGB equations with the NSUR method, respectively; BD_{2SLS}, H_{2SLS} and AGB_{2SLS} are the BD growth, H growth, and AGB equations with 2SLS method, respectively; BD_{3SLS}, H_{3SLS} and AGB_{3SLS} are the BD growth, H growth, and AGB equations with 3SLS method, respectively.

Figure 2 shows the relationships between the observed and fitted values of BD growth, H growth, and AGB models of *C. korshinskii* shrubs according to NLS. The rates of R^2 for the three models were 98.66%, 98.65, and 96.14%.

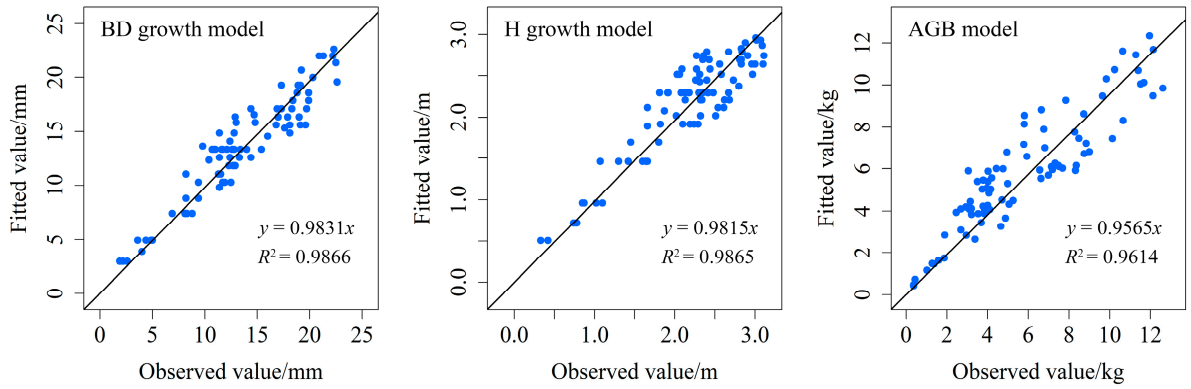

Figure 2. Relationships between the observed and fitted values of BD growth, H growth, and AGB models of *C. korshinskii* shrubs according to the NSUR method of the NLS equation system.

3.3. Models with Heteroscedasticity

Biomass and sample plot data often have measurement errors, as well as individual differences among samples, which models sometimes neglect, thereby leading to heteroscedasticity of the estimated results. In this study, the PF, EF, and CPF were used to eliminate heteroscedasticity. Then, the AIC, BIC, and −2LL were used to compare model performances. The value of −2LL was produced by the log of the LR, which provides a ratio of the probability of correct predictions and incorrect predictions. Results revealed that there were significant differences ($p < 0.0001$) detected between the models with and without heteroscedasticity for BD growth, H growth, and AGB (Table 9). The models that used PF as the variance function had the smallest AIC, BIC, and −2LL for BD growth, H growth, and AGB.

Table 9. Fit of BD growth, H growth, and AGB models with and without heteroscedasticity of *C. korshinskii* shrubs.

Model	Variance Function	AIC	BIC	−2LL	LR	*p*-Value
BD growth	No	370.41	380.27	362.41		
	PF	348.90	361.23	338.91	23.50 [a]	<0.0001
	EF	353.25	365.58	343.25	19.16 [b]	<0.0001
	CPF	350.90	365.70	338.91	23.50 [c]	<0.0001
H growth	No	38.77	48.64	30.77		
	PF	23.43	35.76	13.43	17.34 [a]	<0.0001
	EF	25.91	38.24	15.91	14.86 [b]	<0.0001
	CPF	25.43	40.23	13.43	17.34 [c]	<0.0001
AGB	No	311.80	319.20	305.80		
	PF	275.96	285.82	267.96	37.84 [a]	<0.0001
	EF	296.69	306.56	288.69	17.11 [b]	<0.0001
	CPF	277.96	290.29	267.96	37.84 [c]	<0.0001

Note: [a] LR was calculated with respect to the models without heteroscedasticity and the models using PF as the variance function for the AGB of *C. korshinskii* shrubs. [b] LR was calculated with respect to the models without heteroscedasticity and the models using EF as the variance function for the AGB of *C. korshinskii* shrubs. [c] LR was calculated with respect to the models without heteroscedasticity and the models using CPF as the variance function for the AGB of *C. korshinskii* shrubs.

Figure 3 shows the standardized residuals of the BD growth, H growth, and AGB models, which had poor fit for all shrub components with obvious trends (trumpet residuals). However, the plots of the models with heteroscedasticity using PF as the variance function had better fit and no obvious trends.

3.4. Models Comparisons

Table 10 shows the evaluations of the NLS equation of BD and H growth and AGB of *C. korshinskii* shrubs. The Gompertz equation indicated there was a relationship between the AGB and age and numbers of stems using GNL regression. Results revealed that the *AMR* and *RMSE* of the NLS equation were 1.0514 and 1.3584, which decreased by 22.31% and 19.02%, respectively, when compared to the Gompertz growth equation for AGB. The adj-R^2 was 0.8246 from the NLS equations, which increased by 10.64%. Additionally, we found that the NLS equation greatly improved the model accuracy and reduced forecast estimation errors.

Table 10. Summary of evaluations from the NLS equation of BD and H growth and AGB equations of *C. korshinskii* shrubs. The Gompertz equation indicated there was a relationship between AGB and age using GNL regression.

Equation	Index	*AMR*	*RMSE*	adj-R^2
NLS	BD growth	1.3481	1.8046	0.9055
	H growth	0.2171	0.2683	0.8644
	AGB	1.0514	1.3584	0.8246
Gompertz	AGB	1.2860	1.6168	0.7453

Figure 4 shows the predicted BD growth, H growth, and AGB of *C. korshinskii* shrubs from the NLS equations and predicted AGB versus age and number of stems from the Gompertz equations using GNL regression. There were significant differences between the AGB estimates from the NLS equations and the Gompertz growth equation using GNL regression.

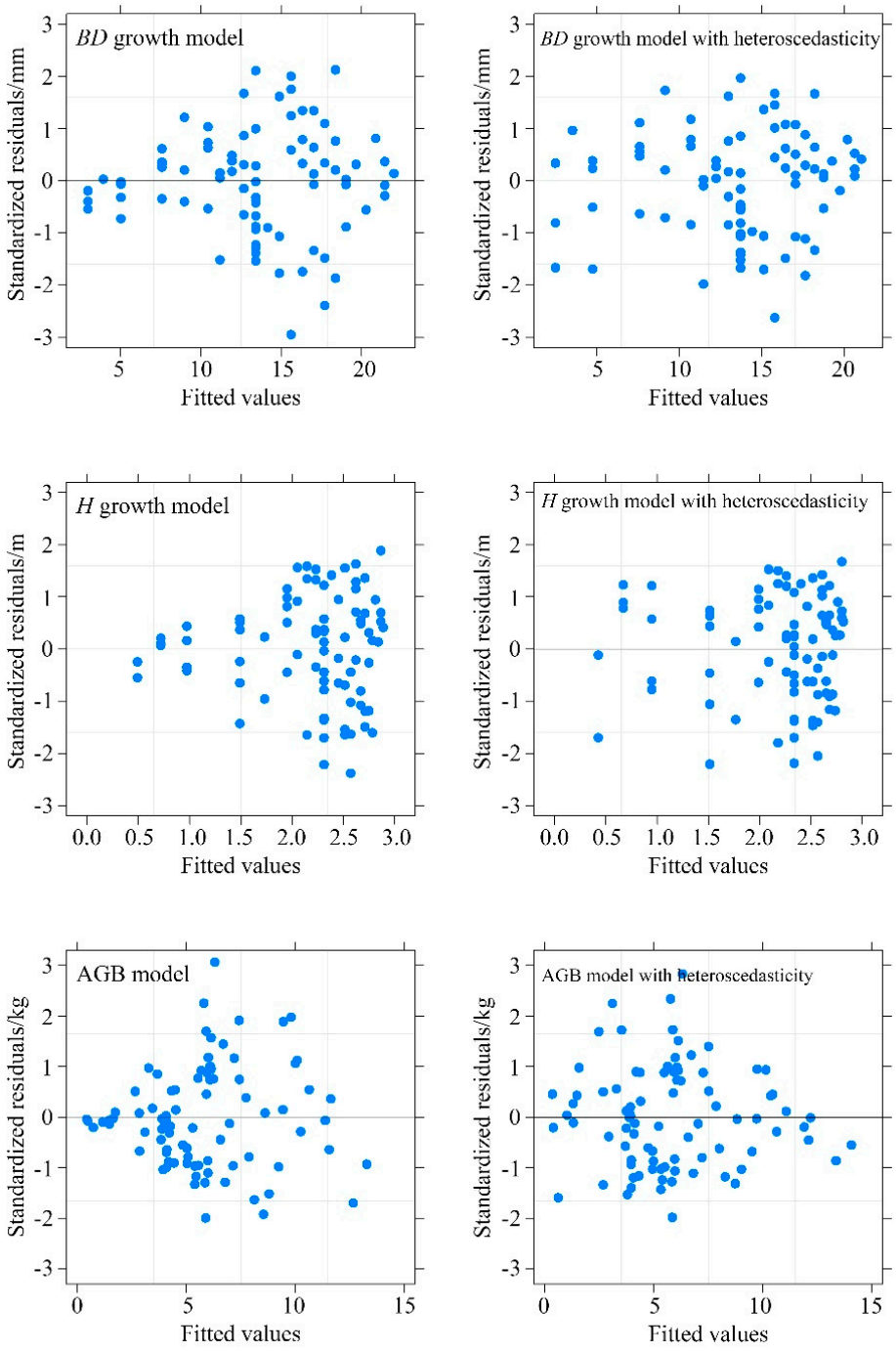

Figure 3. Plots of standardized residuals against fitted values of the BD growth, H growth, and AGB models with and without heteroscedasticity of *C. korshinskii* shrubs according to the NSUR method of the NLS equation system.

The NLS equations system provided a feasible research method for estimating *Caragana* shrub layer biomass; scientifically supported regional ecosystem protection, restoration, and reconstruction; and accurately evaluated ecosystem service functions in the AASRs.

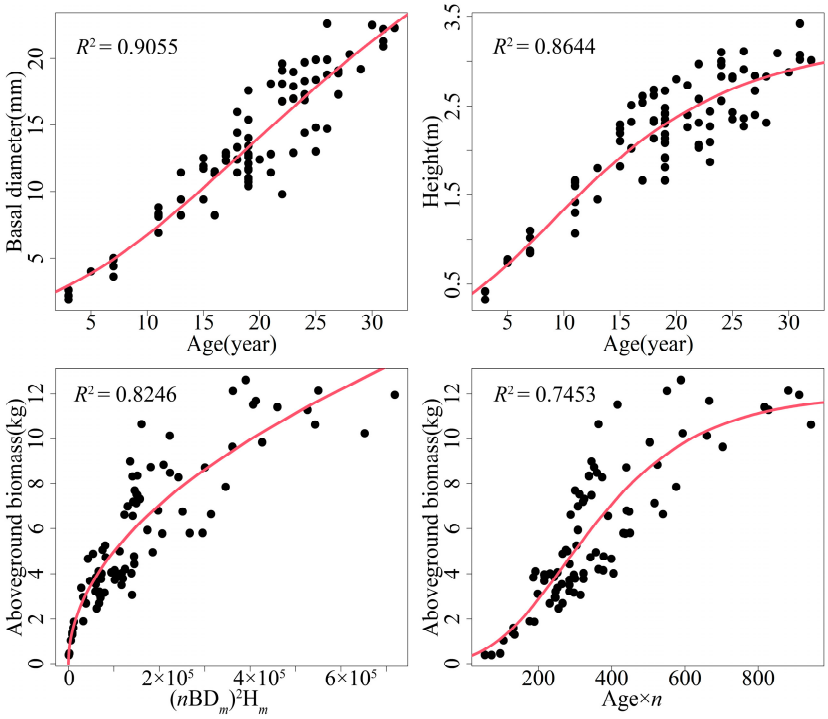

Figure 4. Predicted BD, H, and AGB values of *C. korshinskii* shrubs using the NLS equation and predicted AGB versus age and number of stems by the Gompertz equation using GNL regression. Black dots indicate the observed values.

4. Discussion

As important components of forest resources, shrubs play unique roles in mitigating global climate change [41]. Monitoring shrub biomass and carbon storage has increasingly attracted global attention [3,42]. There are many direct harvesting, model estimation, and remote sensing interpretation methods for obtaining shrub biomass. Although the accuracy of precise harvesting is very high, it requires considerable manpower and material resources and is destructive to the forest. Additionally, it greatly increases the vulnerability of the desert ecosystem and does not contribute to its protection. Advanced methods, such as remote sensing technology and geographic information systems, have irreplaceable advantages in the estimation of forest biomass and net growth on a large and even global scale. However, due to the limitations of remote sensing data in space, spectrum, and radiation resolution, the accuracy of estimating ground forest biomass using remote sensing data is unreliable [43]. Therefore, due to the establishment of shrub biomass prediction models using easily measurable factors, these models have become effective methods for measuring shrub biomass in the AASRs.

In this study, we applied the GNL regression approach [44] to develop TG equations of BD and H on the basis of the Gompertz, Logistic, Mitscherlich, Richards, and Korf equations. Then, the optimal equations for BD and H growth were selected on the basis of the *AMR*, *RMSE*, and adj-R^2 values. The Gompertz equation showed the best performance for both BD and H growth of *C. korshinskii* shrubs (Table 6) [20,45]. Moreover, the $n\mathrm{BD}_m$, $n\mathrm{H}_m$, and $(n\mathrm{BD}_m)^2H_m$ were used as the independent variables to build the AGB AG equation. The equation using $(n\mathrm{BD}_m)^2\mathrm{H}_m$ as the independent variable performed better than the others (Table 7) [10,11,46]. Finally, the NOLS, NSUR, 2SLS, and 3SLS methods of the NLS equations were constructed and combined BD and H growth from the TG equation and AGB from the AG equation (Table 8).

In this study, we found identical fit and evaluation when using the NOLS and GNL regression approach. It also showed the same prediction for the methods of 2SLS and 3SLS. Tang et al. [47] demonstrated that, in some situations, the NOLS is more efficient than the GNL regressions. Despite having a slight lower efficiency, a main advantage

of 2SLS is that this can be estimated consistently with the existence of heteroscedasticity. What is more, there were theoretical advantages for both 2SLS and 3SLS when compared to the NSUR method. However, they required large sample datasets and overidentified estimation, which was difficult to realize in the forest biomass equations [48]. The duration of the equation fittings for the NLS equations methods was ordered as follows: 3SLS (16.87 s) > 2SLS (10.92 s) > NSUR (3.21 s) > NOLS (1.26 s). Therefore, the NSUR method of the NLS equations was determined to have the best performance [49,50].

The NLS equations system could significantly improve the model accuracy and reduce the estimation error of the predictions [23]. The estimation error also met the accuracy requirements on a regional scale; reduced the error between biomass and carbon storage estimation; and could serve as a reference for forest management, the rational utilization of resources, and mitigation of climate change.

As an important component of shrub biomass, AGB accounts for 60–70% of the biomass of an individual shrub [51], while the underground biomass of *C. korshinskii* shrubs accounts for 30–40% of the total shrub biomass [52]. However, the variation in underground biomass growth for *C. korshinskii* shrubs remains unclear. Future studies should focus on identifying variations in shrub biomass to assist with the improvement of shrub biomass estimates when modeling *C. korshinskii* growth.

5. Conclusions

In this study, the NLS equation systems of BD growth, H growth, and AGB models were used to quantify *C. korshinskii* shrub AGB growth on the basis of the theorical growth and allometric growth equations in northwestern China. It was found that the Gompertz equation had better performance than the other equations using GNL regression for the BD and H growth models. For the AGB models, using $(n\mathrm{BD}_m)^2\mathrm{H}_m$ as the independent variable resulted in better evaluations. The NSUR method of the NLS equations had better performance than the other three methods and the independent equations, which thereby provides an efficient method for predicting AGB growth of *C. korshinskii* shrubs. Moreover, the equations with heteroscedasticity accounted for multiple sources of heteroscedasticity found in the data, thus making the NLS equations approach an attractive option for *C. korshinskii* shrub biomass growth estimation. The NLS equations fitted in this study are appropriate for modeling new shrubs that have ecological characteristics and growth features similar to *C. korshinskii* shrubs in the AASRs.

Author Contributions: Conceptualization, H.X. and X.J.; methodology, H.X.; software, X.J.; validation, H.X. and X.J.; formal analysis, X.J.; investigation, B.W. and X.W.; writing—original draft preparation, X.J.; writing—review and editing, H.X.; visualization, X.J.; supervision, H.X. All authors have read and agreed to the published version of the manuscript.

Funding: This research was funded by Ningxia Natural Science Foundation, grant number [2020AAC03089] and Ningxia Natural Science Foundation, grant number [2022AAC03033].

Institutional Review Board Statement: Not applicable.

Informed Consent Statement: Not applicable.

Data Availability Statement: Data available on request due to privacy restrictions. The data presented in this study are available on request from the corresponding author. The data are not publicly available due to be collected by privacy.

Acknowledgments: We thank Yifu Wang (Beijing Forestry University) for his contributions to the data analysis.

Conflicts of Interest: The authors declare no conflict of interest.

Abbreviations

Aboveground biomass	AGB	Arid aeolian sand regions	AASRs
Theoretical growth	TG	Allometric growth	AG
Nonlinear simultaneous	NLS	Generalized nonlinear	GNL
Nonlinear ordinary least square	NOLS	Nonlinear seemingly uncorrelated regression	NSUR
Two-stage least squares	2SLS	Three-stage least squares	3SLS
Basal diameter	BD	Height	H
Absolute mean residual	*AMR*	Root mean system error	*RMSE*
Adjusted determination coefficient	adj-R^2	Power function	PF
Exponential function	EF	Constant plus power function	CPF
Akaike information criterion	AIC	Bayesian information criterion	BIC
Negative two times the logarithm of the likelihood	−2LL		

References

1. Lin, J.; Chen, D.; Wu, W.; Liao, X. Estimating aboveground biomass of urban forest trees with dual-source UAV acquired point clouds. *Urban For. Urban Green.* **2022**, *69*, 127521. [CrossRef]
2. Brahma, B.; Nath, A.J.; Sileshi, G.W.; Das, A.K. Estimating biomass stocks and potential loss of biomass carbon through clear-felling of rubber plantations. *Biomass Bioenergy* **2018**, *115*, 88–96. [CrossRef]
3. Vega, J.A.; Arellano-Pérez, S.; Álvarez-González, J.G.; Fernández, C.; Jiménez, E.; Fernández-Alonso, J.M.; Vega-Nieva, D.J.; Briones-Herrera, C.; Alonso-Rego, C.; Fontúrbel, T.; et al. Modelling aboveground biomass and fuel load components at stand level in shrub communities in NW Spain. *For. Ecol. Manag.* **2022**, *505*, 119926. [CrossRef]
4. Xu, H.; Wang, Z.; Li, Y.; He, J.; Wu, X. Dynamic growth models for *Caragana korshinskii* shrub biomass in China. *J. Environ. Manag.* **2020**, *269*, 110675. [CrossRef]
5. Rafikul, I.M.; Salim, A.M.; Subhan, M.A.; Md, K.; Islam, K.M.N. Allometric equations for estimating stem biomass of *Artocarpus chaplasha* Roxb in Sylhet hill forest of Bangladesh. *Trees For. People* **2021**, *4*, 100084.
6. Fu, L.; Zeng, W.; Tang, S. Individual Tree Biomass Models to Estimate Forest Biomass for Large Spatial Regions Developed Using Four Pine Species in China. *For. Sci.* **2017**, *63*, 241–249.
7. Whittaker, R.H. Net Production Relations of Shrubs in the Great Smoky Mountains. *Ecology* **1962**, *43*, 357–377. [CrossRef]
8. Whittaker, R.H. Estimation of Net Primary Production of Forest and Shrub Communities. *Ecology* **1961**, *42*, 177–180. [CrossRef]
9. Lufafa, A.; Diédhiou, I.; Ndiaye, N.A.S.; Séné, M.; Kizito, F.; Dick, R.P.; Noller, J.S. Allometric relationships and peak-season community biomass stocks of native shrubs in Senegal's Peanut Basin. *J. Arid Environ.* **2009**, *73*, 260–266. [CrossRef]
10. Huff, S.; Ritchie, M.; Temesgen, H. Allometric equations for estimating aboveground biomass for common shrubs in northeastern California. *For. Ecol. Manag.* **2017**, *398*, 48–63. [CrossRef]
11. Randriamalala, J.R.; Radosy, H.O.; Ramanakoto, M.; Razafindrahanta, H.; Ravoninjatovo, J.; Haingomanantsoa, R.S.; Ramananantoandro, T. Allometric models to predict the individual aboveground biomass of shrubs of Malagasy xerophytic thickets. *J. Arid Environ.* **2022**, *202*, 104751. [CrossRef]
12. Conti, G.; Gorné, L.D.; Zeballos, S.R.; Lipoma, M.L.; Gatica, G.; Kowaljow, E.; WhitworthHulse, J.I.; Cuchietti, A.; Poca, M.; Pestoni, S.; et al. Developing allometric models to predict the individual aboveground biomass of shrubs worldwide. *Glob. Ecol. Biogeogr.* **2019**, *28*, 961–975. [CrossRef]
13. Repo, A.; Rajala, T.; Henttonen, H.M.; Lehtonen, A.; Peltoniemi, M.; Heikkinen, J. Age-dependence of stand biomass in managed boreal forests based on the Finnish National Forest Inventory data. *For. Ecol. Manag.* **2021**, *498*, 119507. [CrossRef]
14. Li, Y.; Yuan, L.; Cao, H.; Tang, C.; Wang, X.; Tian, B.; Dou, S.; Zhang, L.; Shen, J. A dynamic biomass model of emergent aquatic vegetation under different water levels and salinity. *Ecol. Model.* **2021**, *440*, 109398. [CrossRef]
15. Xu, H.; Wang, Z.; He, J.; Yu, H. Height growth process of *Caragana korshinskii* based on nonlinear mixed effects models in Yanchi. *J. Northwest AF Univ. Nat. Sci. Ed.* **2017**, *45*, 95–115.
16. Damgaard, C. A Critique of the Space-for-Time Substitution Practice in Community Ecology. *Trends Ecol. Evol.* **2019**, *34*, 416–421. [CrossRef]
17. Yue, C.; Kahle, H.; von Wilpert, K.; Kohnle, U. A dynamic environment-sensitive site index model for the prediction of site productivity potential under climate change. *Ecol. Model.* **2016**, *337*, 48–62. [CrossRef]
18. Ma, J.; Xiao, X.; Bu, R.; Doughty, R.; Hu, Y.; Chen, B.; Li, X.; Zhao, B. Application of the space-for-time substitution method in validating long-term biomass predictions of a forest landscape model. *Environ. Model. Softw.* **2017**, *94*, 127–139. [CrossRef]
19. Lei, Y.; Fu, L.; Affleck, D.L.R.; Nelson, A.S.; Shen, C.; Wang, M.; Zheng, J.; Ye, Q.; Yang, G. Additivity of nonlinear tree crown width models: Aggregated and disaggregated model structures using nonlinear simultaneous equations. *For. Ecol. Manag.* **2018**, *427*, 372–382. [CrossRef]
20. Shoda, T.; Imanishi, J.; Shibata, S. Growth characteristics and growth equations of the diameter at breast height using tree ring measurements of street trees in Kyoto City, Japan. *Urban For. Urban Green.* **2020**, *49*, 126627. [CrossRef]
21. Zeide, B.; Zhang, Y. Diameter variability in loblolly pine plantations. *For. Ecol. Manag.* **2000**, *128*, 139–143. [CrossRef]

22. Giebink, C.L.; DeRose, R.J.; Castle, M.; Shaw, J.D.; Evans, M.E.K. Climatic sensitivities derived from tree rings improve predictions of the Forest Vegetation Simulator growth and yield model. *For. Ecol. Manag.* **2022**, *517*, 120256. [CrossRef]
23. Yang, J.; Cooper, D.J.; Li, Z.; Song, W.; Zhang, Y.; Zhao, B.; Han, S.; Wang, X. Differences in tree and shrub growth responses to climate change in a boreal forest in China. *Dendrochronologia* **2020**, *63*, 125744. [CrossRef]
24. Kašpar, J.; Tumajer, J.; Treml, V. IncrementR: Analysing height growth of trees and shrubs in R. *Dendrochronologia* **2019**, *53*, 48–54. [CrossRef]
25. Ma, J.; Yuan, C.; Zhou, J.; Li, Y.; Gao, G.; Fu, B. Logistic model outperforms allometric regression to estimate biomass of xerophytic shrubs. *Ecol. Indic.* **2021**, *132*, 108278. [CrossRef]
26. Gheyret, G.; Zhang, H.; Guo, Y.; Liu, T.; Bai, Y.; Li, S.; Schmid, B.; Bruelheide, H.; Ma, K.; Tang, Z. Radial growth response of trees to seasonal soil humidity in a subtropical forest. *Basic Appl. Ecol.* **2021**, *55*, 74–86. [CrossRef]
27. Bosela, M.; Lukac, M.; Castagneri, D.; Sedmák, R.; Biber, P.; Carrer, M.; Konôpka, B.; Nola, P.; Nagel, T.A.; Popa, I.; et al. Contrasting effects of environmental change on the radial growth of co-occurring beech and fir trees across Europe. *Sci. Total Environ.* **2018**, *615*, 1460–1469. [CrossRef]
28. Luo, J.; Zhang, M.; Zhou, X.; Chen, J.; Tian, Y. Tree Height and DBH Growth Model Establishment of Main Tree Species in Wuling Mountain Small Watershed. *IOP Conf. Ser. Earth Environ. Sci.* **2018**, *108*, 042003. [CrossRef]
29. Yuancai, L.; Marques, C.P.; Macedo, F.W. Comparison of Schnute's and Bertalanffy-Richards' growth functions. *For. Ecol. Manag.* **1997**, *96*, 283–288. [CrossRef]
30. Dutcă, I.; McRoberts, R.E.; Næsset, E.; Blujdea, V.N.B. Accommodating heteroscedasticity in allometric biomass models. *For. Ecol. Manag.* **2022**, *505*, 119865. [CrossRef]
31. Cheng, X.; Huang, M.; Shao, M.; Warrington, D.N. A comparison of fine root distribution and water consumption of mature *Caragana korshinkii* Kom grown in two soils in a semiarid region, China. *Plant Soil* **2009**, *315*, 149–161. [CrossRef]
32. Xu, J.; Xiao, Y.; Xie, G.; Wang, Y.; Jiang, Y. Computing payments for wind erosion prevention service incorporating ecosystem services flow and regional disparity in Yanchi County. *Sci. Total Environ.* **2019**, *674*, 563–579. [CrossRef]
33. Du, L.; Zeng, Y.; Ma, L.; Qiao, C.; Wu, H.; Su, Z.; Bao, G. Effects of anthropogenic revegetation on the water and carbon cycles of a desert steppe ecosystem. *Agr. For. Meteorol.* **2021**, *300*, 108339. [CrossRef]
34. Li, B.; Gao, J.; Wang, X.; Ma, L.; Cui, Q.M. Effects of biological soil crusts on water infiltration and evaporation Yanchi Ningxia, Maowusu Desert, China. *Int. J. Sediment Res.* **2016**, *31*, 311–323. [CrossRef]
35. Long, Y.; Liang, F.; Zhang, J.; Xue, M.; Zhang, T.; Pei, X. Identification of drought response genes by digital gene expression (DGE) analysis in Caragana korshinskii Kom. *Gene* **2020**, *725*, 144170. [CrossRef]
36. Wang, B.; Zhao, X.; Liu, Y.; Fang, Y.; Ma, R.; Yu, Q.; An, S. Using soil aggregate stability and erodibility to evaluate the sustainability of large-scale afforestation of *Robinia pseudoacacia* and *Caragana korshinskii* in the Loess Plateau. *For. Ecol. Manag.* **2019**, *450*, 117491. [CrossRef]
37. Lu, D.; Chen, Q.; Wang, G.; Liu, L.; Li, G.; Moran, E. A survey of remote sensing-based aboveground biomass estimation methods in forest ecosystems. *Int. J. Digit. Earth* **2016**, *9*, 63–105. [CrossRef]
38. Xiuhong, L.; Chunqian, J.; Rui, X.; Xiao, H.; Mengjuan, Q. Comparison of methods to construct compatible individual tree biomass models—A case study of *Cyclobalanopsis glauca*. *Sci. Silvae Sin.* **2020**, *56*, 164–173.
39. Rose, C.E.; Lynch, T.B. Estimating parameters for tree basal area growth with a system of equations and seemingly unrelated regressions. *For. Ecol. Manag.* **2001**, *148*, 51–61. [CrossRef]
40. Haichuan, Z. Air pollution and public health: Evidence from forests absorb smoke and dust emission in China. *Sci. Silvae Sin.* **2017**, *53*, 120–131.
41. Gratani, L.; Catoni, R.; Varone, L. *Quercus ilex* L. carbon sequestration capability related to shrub size. *Environ. Monit. Assess* **2010**, *178*, 383–392. [PubMed]
42. Chang, Q.; Zwieback, S.; DeVries, B.; Berg, A. Application of L-band SAR for mapping tundra shrub biomass, leaf area index, and rainfall interception. *Remote Sens. Environ.* **2022**, *268*, 112747. [CrossRef]
43. Zhu, Y.; Feng, Z.; Lu, J.; Liu, J. Estimation of Forest Biomass in Beijing (China) Using Multisource Remote Sensing and Forest Inventory Data. *Forests* **2020**, *11*, 163. [CrossRef]
44. Zhou, H.; Li, Z.; Liu, W. Connotation analysis of parameters in the generalized nonlinear advection aridity model. *Agric. For. Meteorol.* **2021**, *301–302*, 108343. [CrossRef]
45. Estrada, E.; Bartesaghi, P. From networked SIS model to the Gompertz function. *Appl. Math. Comput.* **2022**, *419*, 126882. [CrossRef]
46. Flade, L.; Hopkinson, C.; Chasmer, L. Allometric Equations for Shrub and Short-Stature Tree Aboveground Biomass within Boreal Ecosystems of Northwestern Canada. *Forests* **2020**, *11*, 1207. [CrossRef]
47. Tang, S.; Li, Y.; Wang, Y. Simultaneous equations, error-in-variable models, and model integration in systems ecology. *Ecol. Model.* **2001**, *142*, 285–294. [CrossRef]
48. Yang, Z.; Liu, Q.; Luo, P.; Ye, Q.; Duan, G.; Sharma, R.P.; Zhang, H.; Wang, G.; Fu, L. Prediction of Individual Tree Diameter and Height to Crown Base Using Nonlinear Simultaneous Regression and Airborne LiDAR Data. *Remote Sens.* **2020**, *12*, 2238. [CrossRef]
49. Nord-Larsen, T.; Meilby, H.; Skovsgaard, J.P.; Sveriges, L. Simultaneous estimation of biomass models for 13 tree species: Effects of compatible additivity requirements. *Can. J. For. Res.* **2017**, *47*, 765–776. [CrossRef]

50. Fu, L.; Lei, Y.; Zeng, W. Comparison of Several Compatible Biomass Models and Estimation Approaches. *Sci. Silvae Sin.* **2014**, *50*, 42–54.
51. Huang, C.; Feng, C.; Ma, Y.; Liu, H.; Wang, Z.; Yang, S.; Wang, W.; Fu, S.; Chen, H.Y.H. Allometric models for aboveground biomass of six common subtropical shrubs and small trees. *J. For. Res.* **2021**, *33*, 1317–1328. [CrossRef]
52. Wang, G.; Chen, Z.; Yang, X.; Cai, G.; Shen, Y. Effect of simulated precipitation regimes on sap flow and water use efficiency for xerophytic *Caragana korshinskii*. *Ecol. Indic.* **2022**, *143*, 109309. [CrossRef]